Charge Driven Fragmentation of Nucleobases

J. de Vries, R. Hoekstra, R. Morgenstern, and T. Schlathölter*

KVI Atomic Physics, Rijksuniversiteit Groningen, Zernikelaan 25, 9747AA Groningen, The Netherlands

(Received 6 February 2003; published 31 July 2003)

We studied multiple ionization of single nucleobases by means of slow highly charged ions (Xe^{q+}, $q = 5$–25). The products of the subsequent fragmentation were studied using high resolution coincidence time-of-flight spectrometry. We observed a strong dependence of the fragment kinetic energies on the initial charge state of the intermediate parent ions as well as on the initial chemical environment of the respective fragment ions within the parent molecule. The data allow us to shed light on the charge distribution within the molecule as well as on the fragmentation dynamics of these intermediate size systems.

DOI: 10.1103/PhysRevLett.91.053401 PACS numbers: 36.40.Qv, 34.70.+e, 36.40.Wa, 87.50.Gi

The effect of ionizing radiation on cells is by and large due to damage of the cellular DNA [1]. Within the track of the primary radiation, secondary particles such as electrons and (singly/multiply charged) ions are formed. It is, e.g., the interaction of these ions with biologically relevant structures such as DNA which causes major biological damage. Multiply charged heavy ions as primary particles are of importance in cancer therapy and radiation exposure of astronauts. Cross sections for the involved collision systems are necessary for correct quantitative considerations of radiation damage. Until now, mechanisms of radiation damage have been studied only for the mesoscopic scale of biological systems and not on the single molecule level.

Ionization and fragmentation of isolated gas-phase nucleobases has received only little interest at all. Dissociative electron attachment to DNA bases [2], uracil [3], as well as bromouracil [4,5] showed how even resonant capture of electrons at kinetic energies well below the ionization energy induces substantial fragmentation. The direct importance of these electrons in DNA strand breaking has been demonstrated very recently [6]. Fragmentation of gas-phase uracil by means of keV protons has been investigated as well [3] and similarities to electron impact experiments were observed.

Here we focus on the interaction of nucleobases with the electric field of a slow highly charged ion (HCI). Such fields are comparable to those of fs lasers in the sense that field duration ($\approx$ fs) and strength ($\approx 10^{10}$ V/m) are comparable. HCI-induced ionization and fragmentation of diatomic and triatomic molecules are understood in great detail. The fragmentation dynamics can be investigated beyond the limit of pure Coulomb explosion models. In studies on CO, various excited molecular states were found to contribute and it was proven that predominantly valence electrons are removed without strong excitation of the molecule [7,8]. For fast HCI, Siegmann *et al.* [9] also had to invoke the potential energy curves of excited states to explain the kinetic energy distributions of N_2 fragments observed after interaction with fast HCI. For extremely low collision velocities, even the presence of the highly charged ion strongly affects the fragmentation process [10,11].

The response of large systems such as clusters upon the electric field of a multiply charged ion has been studied with great interest as well. The complexity of the problem, i.e., the many-body nature of the cluster, calls for statistical approaches. In particular, C_{60} has drawn a lot of attention [12–15], but studies on metal [16–18] and van der Waals clusters [19] have also been performed.

The response of intermediately sized molecules, which might bridge the gap between small molecules and large clusters, to strong electric fields has barely been investigated. Several of these systems share properties with large entities such as C_{60}, e.g., delocalized π electrons. The interaction of fast HCI as well as strong laser fields with benzene molecules has been studied by Mathur [20], and, despite several orders of magnitude difference in excitation time, the observed fragmentation patterns are similar. This might indicate a statistical redistribution of the energy before fragmentation takes place. On the other hand, for C^{q+} interaction with uracil the electronic structures of both ion and molecule play a crucial role in the interaction dynamics [21].

In the following, we discuss the issue of energetic nucleobase fragments which could cause subsequent damage in biological systems. We also focus on fundamental issues such as charge distribution within the intermediate multiply charged molecular complex, fragmentation dynamics, and the influence of the molecular geometry on the coincidence patterns.

The experimental setup has been described in detail before [21]. Briefly, $^{129}Xe^{q+}$ ($q = 5$–25) ions are extracted from the electron cyclotron resonance ion source located at the KVI in Groningen. The source is floated on potentials ranging from 5 to 25 kV to obtain $v = 0.2$ a.u. for all charge states. In the collision chamber, the ion beam is crossed with a gaseous target of either uracil or thymine, evaporated from an oven at 180 and 170 °C, respectively. Uracil ($M = 112$ amu) is based on

a six-membered ring consisting of C and N atoms with H and O atoms attached to it. In case of thymine ($M = 126$ amu), one H atom is replaced by a methyl group. The molecules effuse through a 500 μm nozzle placed ≈ 20 mm from the collision center. The base pressure during experiments is kept below 1×10^{-8} mbar. A static electric field of 600 V/cm extracts charged particles from the collision region. These ions are guided into a reflectron time-of-flight (TOF) spectrometer (resolution $\Delta m/m = 1500$ at $m = 720$ amu [22]) and detected on a multisphere plate (MSP) detector. Opposite to the fragment ions, electrons, used to start the TOF measurement, are extracted through a 5 mm diaphragm onto an MSP. For each start, several fragment ions can be detected in coincidence (dead time ≈ 50 ns) and analyzed in an event-by-event mode. A more detailed description can be found in [23].

Figure 1 displays a mass spectrum of uracil fragments after ionization by Xe^{14+}. (The structure of uracil as well as theymine is depicted in Fig. 2. Uracil is based on a six-membered ring consisting of C and N atoms with H and O atoms attached to it. In case of thymine, one H atom is replaced by a methyl group.) This electron-ion coincidence spectrum is typical for the systems studied here: small fragments prevail, with maximum intensities at H^+ and C^+. With increasing q the fragment distribution centers even more at small fragments. Single ionization events are discriminated because of the absence of an emitted electron capture event. Only direct single ionization, a weak channel at low energies, leads to electron emission. Therefore, the detection of singly charged large fragments and intact molecules is strongly suppressed [23]. The low mass region shown in Fig. 1 is basically unaffected by the coincidence requirement. The inset shows a zoom of the doubly charged ion region: For O^{2+} and N^{2+} (as for the corresponding singly and triply charged ions), we observe a clear double structure. This is due to the limited transmission of the system for (fragment) ions formed with high kinetic energy. Ions emitted perpendicular to the detection axis are intercepted by diaphragms, i.e., forward and backward emitted ions

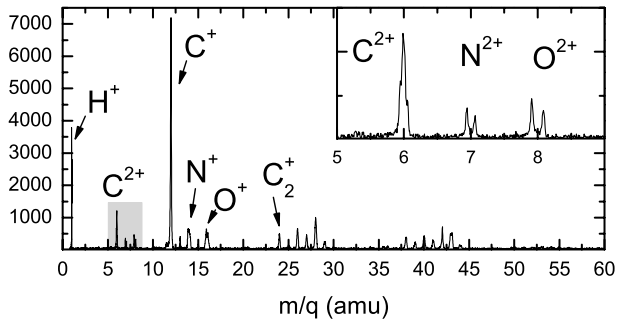

FIG. 1. Electron-ion coincidence mass spectrum for interaction of $^{129}Xe^{14+}$ interacting with uracil. The inset shows the shaded region of doubly charged fragment ions.

contribute strongest. As opposed to N^{r+} and O^{r+}, for C^{r+} the peaks are much narrower, indicating a small kinetic energy. The C^{r+} transmission is therefore higher and the respective branching ratio of the ion yields $[C^{r+}/(C^+ + C^{2+} + C^{3+})]$, a good measure for the actual charge on the parent molecule. (Throughout this Letter, q is used for the projectile charge state, r for fragment ions, and s for the charge state of the intermediate parent molecule.)

For the molecules under study these branching ratios are displayed as a function of q in Fig. 2. Multiply charged carbon ions are insignificant for $q < 10$. Above $q = 10$ a dramatic increase of C^{2+} sets in, saturating for $q \geq 20$. Even though the general trends are identical for the two molecules under study, the onset and maximum values of the curves depend strongly on the molecular size which defines the total charge the fragments all together can accommodate. For uracil (12 atoms) the branching ratio for C^{2+} is 5% already at $q \approx 10$ and the maximum value is $\approx 35\%$ at $q = 25$. For thymime (15 atoms) C^{2+} reaches 5% at $q = 11$ and reaches a maximum of 28% at $q \approx 25$. In general, for $q > 10$ the regime of complete ionization of the molecular constituents is accompanied by increasing double and triple ionization of the atomic fragments.

How does this transition to complete ionization affect the fragmentation dynamics? The complete ion-ion correlation plots consist of hundreds of ion pairs and are thus difficult to evaluate [23]. Multiple ionization always leads to proton emission early in the fragmentation [24],

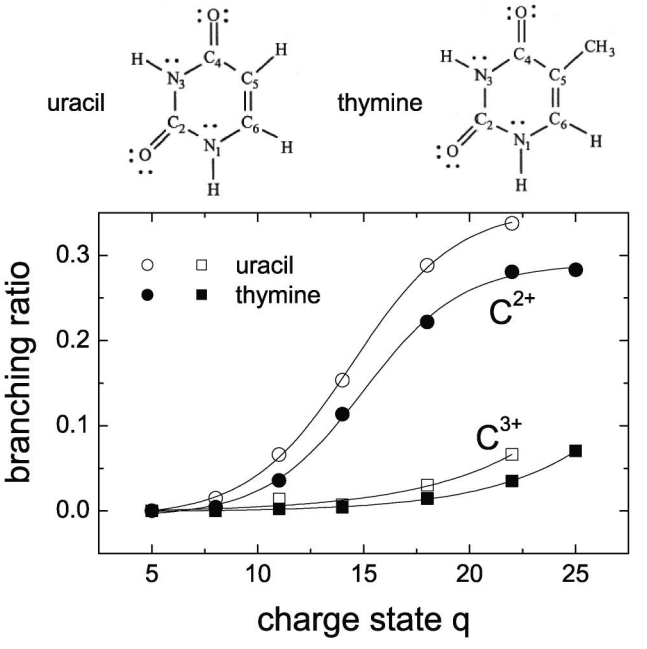

FIG. 2. Branching ratios for the charge states of atomic carbon ions as a function of the projectile q and for uracil and thymine. The lines are sigmoidal fits to the data. Shown above is the structure of the molecules.

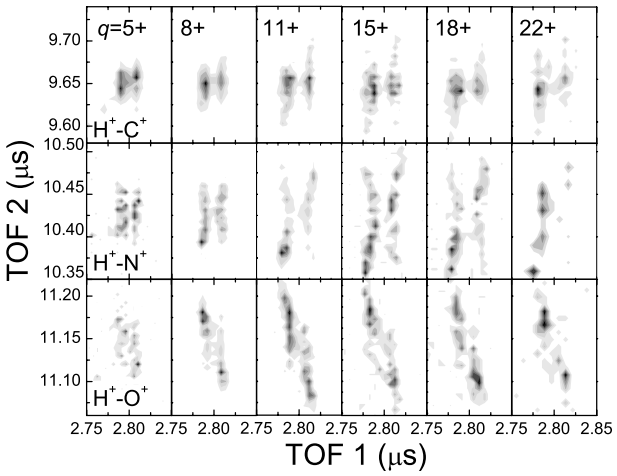

FIG. 3. Contour plots of the correlated flight times for triple coincidences of uracil fragments. Top row: e^-–H^+–C^+; middle row: e^-–H^+–N^+; bottom row: e^-–H^+–O^+. The respective projectile charge state (5 + –22 +) is indicated in the top row. TOF1 relates to H^+ and TOF2 to the heavier ion.

whereas heavier atomic ions are formed when the molecules break up entirely. The correlated flight-time plots in Fig. 3 for the chosen uracil fragmention pairs H^+–C^+, H^+–N^+, and H^+–O^+ (electron–ion–ion coincidence mode) therefore contain complementary information. The shapes of the islands reveal information on the momenta of the correlated fragments. Ideally for two-body breakup the islands are strip-shaped and inclined under 45°. The presence of further bodies changes this angle, since undetected fragments carry away momentum. Deviations from the strip shape have mainly two reasons: (i) The transmission of the TOF system is lower than 100%, because of the system optimization for time-resolution and high fragmention kinetic energies up to around 100 eV. Ions emitted perpendicular to the detector axis are thus discriminated and a gap in the middle of the coincidence islands is induced. Only ions emitted forward (short TOF) and backward (long TOF) are detected. (ii) The TOF measurement is triggered by an emitted electron. For those electrons emitted from the molecule, emission can be assumed to be mainly in the plane of the molecule. This orientation contributes most, thus enhancing the transmission effect.

The ion pairs in Fig. 3 differ from the simple two-body case, since they are due to (possibly multistep) multifragmentation processes. For $q = 5$ all three combinations exhibit similar features, namely, a splitting along the H^+ axis and a broad distribution along the heavy-ion axis. Apparently, first the proton is emitted from a largely intact ring—either towards the detector or away from it. Subsequently, the remaining ring breaks apart into atomic and molecular fragments with statistically distributed energies. This scenario implies the ring fragmentation time scale to be longer than typical molecular vibrations: energy can equilibrate before ring breakup. Atomic ions are formed late in the cascade and have low averaged kinetic energies.

Already at $q = 8$ the island shapes start to develop differently and doubly charged ions start to become important (see Fig. 2). In the C^+ case, the islands' center of gravity does not change. The short TOF1 island, however, gets extended to short TOF2, whereas the long TOF1 island gets extended to long TOF2. This implies that the H^+ and C^+ tend to be emitted in one direction. For the N^+ case, an X-shaped double island develops. The most intense part consists of an extension into short TOF1/short TOF2 and long TOF1/long TOF2 direction as for C^+. However, fragment emission in opposite directions is also observed. For O^+, the island develops in a completely different manner: only the short/long and long/short combinations are found for higher q, indicating that only emission of H^+ and O^+ in opposite directions is observed. Islands of proton coincidences with doubly charged atomic ions (not shown here) appear around $q = 10$ and exhibit the same trends. (For larger fragments the island shapes do not change considerably with q and stay similar to the $q = 5$ islands in Fig. 3.) This can be explained by the geometry of the molecule and the position of the different atoms within: In uracil, the O atoms are on an axis with an H atom on the opposite side of the ring. Thus, only emission in opposite directions is possible. For N and C, half of the atoms are paired with an H on the same side of the molecule, the other half is paired with one H on the same side and one on the opposite side. Emission into the same direction is thus more significant

To understand the difference between the H^+–C^+ and H^+–N^+ island shapes, we extracted the maximum kinetic energy (above which 10% of the events are found) for each fragment of the respective pair from the correlation plots. Figure 4 shows the results for the uracil ion pairs from Fig. 3 and the respective thymine data. The proton data are displayed in Fig. 4(a), the heavy-ion data in Fig. 4(b). From Fig. 4(a) it is obvious that for H^+–C^+ and for H^+–N^+ the proton kinetic energies are comparable and increase with q. Even at $q = 22$ saturation is not reached. Here we observe the first step of the fragmentation

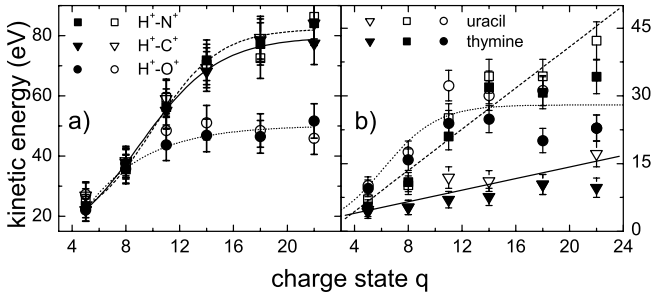

FIG. 4. Maximum kinetic energies for the fragment pairs from Fig. 3 (H^+–C^+: triangles, solid line; H^+–N^+: squares, dashed line; H^+–O^+: circles, dotted line). (a) Proton; (b) heavy ion.

cascade: proton emission from the multiply charged remaining molecular complex. The proton kinetic energy increases with average charge state s of the intermediate complex. For H^+–O^+ pairs the proton energy saturates already around $q = 11$ and reaches a value of ≈ 45 eV. This indicates that for $q > 10$ the O fragments tend to be doubly charged, i.e., oxygen seems to attract positive charge. An explanation could be Coulomb repulsion forcing the positive charges to occupy the outermost sites in the molecular complex . The kinetic energy of the O^+ itself [Fig. 4(b)] exhibits a similar saturation and reaches a value of about 30 eV. This can be explained qualitatively by the same argument. However, the kinetic energy of the C^+ and N^+ ions differs by a factor of 3 even though the respective protonic partners had comparable energies. Clearly, now we are watching a later step of the fragmentation cascade. Both ions stem from the ring itself. We explain the energy difference to be due partly to their environment within the parent molecule: as obvious from Fig. 2, two of the C constituents of uracil attached to the O atoms are located in the center triangle of three heavy atoms O, N, and C. Resulting C^+ ions are blocked when trying to escape.

For a qualitative understanding we performed a straightforward simulation of uracil breakup: the ionized uracil constituents are assumed to interact via Coulomb repulsion only. Time evaluation of the system is followed by solving the ions equations of motion numerically. The results predict the same proton kinetic energy distributions for all four initial H positions within the molecule. Furthermore, no saturation of the O^+ kinetic energy is found but the simulated energies agree well for $s \leq 11$. Apparently, larger s values always require both O atoms to be doubly charged as already indicated before, i.e., the O^+ channel closes. N^+ and C^+ behave qualitatively similar with the exception of the C^+ originating from the blocked sites. Here maximum kinetic energies as low as 5 eV are observed. This not only fits to our observations but also justifies the use of the C'^+ data to obtain the branching ratios from Fig. 2.

In conclusion, we have studied strong field-induced ionization and fragmentation channels of nucleobases that involve fragmention production and electron emission. For moderate ionization ($q \approx 5$) the fragmentation is a multistep process. Prompt emission of protons is followed by heavier fragments from the subsequent fragmentation cascade. Fragment kinetic energies can exceed 20 eV. Already for $q = 8$ the critical charge for the multistep process seems to be passed and prompt complete Coulomb fragmentation occurs. In this region, charge accumulates outside of the ring: the O atoms are the first constituents observed doubly charged. Protons with up to ≈ 80 eV are formed and the coincidence pattern shapes strongly depend on the molecular geometry and composition. The extraction of absolute cross sections for the various channels remains a future task, though, requiring means for target vapor pressure determination as well as a high transmission detection system.

We gratefully acknowledge financial support from the Stichting voor Fundamenteel Onderzoek der Materie (FOM) which is supported by the Nederlandse Organisatie voor Wetenschapelijk Onderzoek (NWO). T. S. acknowledges support by the Royal Netherlands Academy of Arts and Sciences.

*Electronic address: tschlat@kvi.nl

[1] C. von Sonntag, *The Chemical Basis for Radiation Biology* (Taylor and Francis, London, 1987).
[2] M. A. Huels, I. Hahndorf, E. Illenberger, and L. Sanche, J. Chem. Phys. **108**, 1309 (1998).
[3] B. Coupier *et al.*, Eur. Phys. J. D **20**, 459 (2002).
[4] H. Abdoul-Carime, M. A. Huels, F. Brüning, E. Illenberger, and L. Sanche, J. Chem. Phys. **113**, 2517 (2000).
[5] S. Gohlke and E. Illenberger, Europhys. News **33**, 207 (2002).
[6] B. Boudiaffa, P. Cloutier, D. Hunting, M. A. Huels, and L. Sanche, Science **287**, 1658 (2000).
[7] M. Tarisien *et al.*, J. Phys. B **33**, L11 (2000).
[8] H. O. Folkerts, R. Hoekstra, and R. Morgenstern, Phys. Rev. Lett. **77**, 3339 (1996).
[9] B. Siegmann, U. Werner, R. Mann, N. M. Kabachnik, and H. O. Lutz, Phys. Rev. A **62**, 022718 (2000).
[10] P. Sobocinski *et al.*, J. Phys. B **35**, 1353 (2002).
[11] R. DuBois *et al.*, Europhys. Lett. **49**, 41 (2000).
[12] S. Martin, L. Chen, A. Denis, and J. Desesquelles, Phys. Rev. A **57**, 4518 (1998).
[13] T. Schlathölter, R. Hoekstra, and R. Morgenstern, J. Phys. B **31**, 1321 (1998).
[14] B. Walch, C. L. Cocke, R. Voelpel, and E. Salzborn, Phys. Rev. Lett. **72**, 1439 (1994).
[15] H. Cederquist *et al.*, Phys. Rev. A **61**, 022712 (2000).
[16] F. Chandezon *et al.*, Phys. Rev. Lett. **74**, 3784 (1995).
[17] C. Guet *et al.*, Z. Phys. D **40**, 317 (1997).
[18] L. Plagne and C. Guet, Phys. Rev. A **59**, 4461 (1999).
[19] W. Tappe, R. Flesch, E. Rühl, R. Hoekstra, and T. Schlathölter, Phys. Rev. Lett. **88**, 143401 (2002).
[20] D. Mathur, Phys. Rev. A **63**, 032502 (2002).
[21] J. de Vries, R. Hoekstra, R. Morgenstern, and T. Schlathölter, J. Phys. B **35**, 4373 (2002).
[22] O. Hadjar, R. Hoekstra, R. Morgenstern, and T. Schlathölter, Phys. Rev. A **63**, 033201 (2001).
[23] J. de Vries, R. Hoekstra, R. Morgenstern, and T. Schlathölter, Eur. Phys. J. D (to be published).
[24] S. Shimizu *et al.*, J. Chem. Phys. **117**, 3180 (2002).